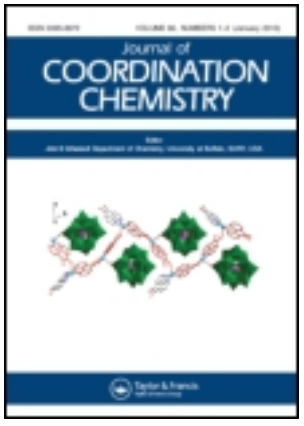

Journal of Coordination Chemistry
Publication details, including instructions for authors and subscription information:
http://www.tandfonline.com/loi/gcoo20

Copper(II) thiocyanate complexes of 2-(2-pyridinyl)-benzthiazole: synthesis, structure, redox behavior, thermal aspects, and DFT calculations

Shubhamoy Chowdhury[a], Smita Majumder[a], Arnab Bhattacharya[a], Partha Mitra[b] & Jnan Prakash Naskar[c]

[a] Department of Chemistry, Tripura University, Suryamaninagar, India

[b] Department of Inorganic Chemistry, Indian Association for the Cultivation of Science, Kolkata, India

[c] Department of Chemistry, Inorganic Chemistry Section, Jadavpur University, Kolkata, India

Accepted author version posted online: 02 Sep 2013.Published online: 22 Oct 2013.

To cite this article: Shubhamoy Chowdhury, Smita Majumder, Arnab Bhattacharya, Partha Mitra & Jnan Prakash Naskar (2013) Copper(II) thiocyanate complexes of 2-(2-pyridinyl)-benzthiazole: synthesis, structure, redox behavior, thermal aspects, and DFT calculations, Journal of Coordination Chemistry, 66:19, 3365-3379, DOI: 10.1080/00958972.2013.839784

To link to this article: http://dx.doi.org/10.1080/00958972.2013.839784

Journal of Coordination Chemistry, 2013
Vol. 66, No. 19, 3365–3379, http://dx.doi.org/10.1080/00958972.2013.839784

Copper(II) thiocyanate complexes of 2-(2-pyridinyl)-benzthiazole: synthesis, structure, redox behavior, thermal aspects, and DFT calculations

SHUBHAMOY CHOWDHURY*†, SMITA MAJUMDER†, ARNAB BHATTACHARYA†, PARTHA MITRA‡ and JNAN PRAKASH NASKAR*§

†Department of Chemistry, Tripura University, Suryamaninagar, India
‡Department of Inorganic Chemistry, Indian Association for the Cultivation of Science, Kolkata, India
§Department of Chemistry, Inorganic Chemistry Section, Jadavpur University, Kolkata, India

(*Received 21 June 2013; accepted 1 August 2013*)

Reaction of 2-(2-pyridinyl)-benzthiazole (Pbt), KSCN, and copper(II)perchlorate hexahydrate in 1 : 2 : 1 molar proportion in dimethyl sulfoxide gives monomeric [Cu(Pbt)$(SCN)_2$DMSO] (**1a**). In another run, identical proportions of the same reactants in methanol generates a symmetric thiocyanate bridged dimeric copper(II) compound, [$Cu_2$$(Pbt)_2$$(SCN)_2$] (**2a**), in 72% yield. Both **1a** and **2a** have been characterized by C, H, and N microanalyses, copper estimation, FTIR, UV–vis spectra, and room temperature magnetic susceptibility measurements. The X-ray crystal structures of **1a** and **2a** have been determined. Electrochemical studies of **1a** and **2a** show Cu(II) to Cu(III) oxidation in solution. The thermal behaviors of **1a** and **2a** have been studied. Bond valence sum method of analysis was performed to assign the oxidation state for each copper center in **1a** and **2a**. Geometry optimization of **1a**, **2a,** and their linkage isomers has also been performed at the level of the density functional theory to show that **1a** and **2a** are the most stable congeners. These results corroborate our experimental findings.

Keywords: Copper; Thiocyanate; Electrochemistry; Thermal behavior; DFT calculation

1. Introduction

2-(2-Pyridinyl)-benzthiazole (Pbt) is ubiquitous in various compounds. Owing to its unique structural and physiological properties, Pbt has attracted renewed interest for possible application in electroluminescent devices [1]. Biologically active platinum complexes of Pbt are potential alternatives of cis-platin as anticancer agents [2]. The former oral drugs are more effective with diminished side effects. [Cu(Pbt)Br_2] is an illustrative example of a self-activated DNA damaging agent having promising application in cancer chemotherapy [3]. Oxorhenium(V) and oxotechnetium(V) complexes of Pbt serve as preliminary models for the development of radiopharmaceuticals. These drugs are used for tumor imaging

*Corresponding authors. Email: s.chowdhury@tripurauniv.in (S. Chowdhury); jpnaskar@rediffmail.com (J.P. Naskar)

and/or radiotherapeutic purpose and in the diagnosis of Alzheimer's disease [1, 4, 5]. Apart from biological perspectives, compounds of Pbt have industrial importance. [Pd(Pbt)Cl_2] exhibits catalytic activity toward the Mizoroki-Heck reaction [6]. Photocatalytic studies on a binuclear Ru(II)–Co(II) complex with Pbt were carried out earlier in acidified acetonitrile to demonstrate constant hydrogen generation for a period longer than 42 h [7]. Binding and transfer of molecular dioxygen through mediation of metal complexes with Pbt have been described [8]. [$ReOCl_3$(pbt)] is capable of activating dioxygen and transferring it for further chemical transformations [8]. Consequently, the coordination chemistry of the metal ions with Pbt is vast. Pbt has been extensively used to stabilize metal ions like Fe(II), Co(II), Ni(II), Cu(II), Pd(II), Pt(II), Ru(II), Ru(III), and Re(V) [4, 5, 9–15].

These aspects of Pbt chemistry have kindled our interest. Herein, we report the syntheses, structures, electrochemistry, and theoretical studies at the level of density functional theory (DFT) of a monomeric and dimeric Cu(II) thiocyanate complexes with Pbt. The dimeric thiocyanate bridged copper(II) complex displays a two-step sequential metal centered one-electron oxidation.

2. Experimental

2.1. *Materials and measurements*

All chemicals were of analytical reagent grade and used without purification. Pyridine-2-carboxaldehyde and *o*-aminobenzenethiol were procured from Sigma-Aldrich, USA. Copper was estimated gravimetrically as CuSCN. Microanalyses were performed with a Perkin–Elmer 2400II elemental analyzer. FTIR spectra in the solid phase were recorded as KBr pellets with a Perkin-Elmer FTIR-100 spectrophotometer. UV–vis absorption spectra of **1a** and **2a** were recorded on a Perkin-Elmer Lambda 25 spectrophotometer. Solution conductivity measurements were carried out in DMSO for **1a** and in acetonitrile for **2a** at room temperature on a Systronics (India) direct reading conductivity meter (Model: 304). Cyclic voltammetric (CV) data were acquired on a Bioanalytical Systems Inc. Epsilon electrochemical workstation (Model: CV-50) on a C3 cell stand at 293 K. Dry and degassed DMSO solution for **1a** and acetonitrile solution for **2a**, each of which contained ~1.0 mM of analyte and 0.10 M tetra-*n*-butylammonium perchlorate (TBAP) as supporting electrolyte, were saturated with nitrogen for 15 min prior to each acquisition. A blanket of nitrogen was maintained throughout the measurements. The measurements were carried out with a three-electrode assembly of a glassy carbon (GC) working electrode, a platinum wire counter electrode, and a Ag/AgCl reference electrode. The working electrode was polished before each experiment with alumina slurry. All potentials reported herein are referenced to Ag/AgCl. Thermal analyzes (TGA/DTA) were performed under a dynamic nitrogen atmosphere (20 mL/min) on a Perkin–Elmer instrument (Model: Pyris Diamond TG/DTA). Magnetic susceptibility was determined at room temperature with a Sherwood Scientific Magnetic Susceptibility Balance, Model Auto, and Revision 1.4.0. The magnetometer was calibrated with Hg[$Co(SCN)_4$] and the susceptibility data were corrected for diamagnetism using Pascal's constants.

Caution! Perchlorate salts of metal complexes can be explosive [16]. Although no detonation tendencies have been observed, care is advised and handling of only small quantities recommended.

2.2. *Preparation of metal complexes*

2.2.1. Preparation of [Cu(Pbt)(NCS)$_2$(DMSO)] (1a). 106 mg (0.5 mM) of Pbt and 97 mg (1.0 mM) of KSCN were taken in 20 mL of DMSO. The solution was colorless. About 185 mg (0.5 mM) of $Cu(ClO_4)_2 \cdot 6H_2O$ was dissolved in 5 mL of DMSO and added dropwise with constant stirring to the ligand solution. At the end of addition, a yellow solution was obtained and stirring was continued for another 3 h. After stirring, the resulting reaction mixture was left in air for slow evaporation. After seven days, a crystalline, dark yellow compound was obtained. It was filtered, washed successively with 10 mL of methanol and 10 mL of diethyl ether and then dried in a vacuum desiccator over fused $CaCl_2$. Yield: 160 mg (68%). $C_{16}H_{14}CuN_4OS_4$ (469.65): Anal. Calc for $C_{16}H_{14}CuN_4OS_4$: C, 40.88; H, 3.00; N, 11.92; Cu, 13.53. Found: C, 40.52; H, 3.13; N, 12.08; Cu, 13.19%. FTIR (KBr): ν [cm^{-1}]: 2101(vs) [ν(C≡N)], 2080(vs) [ν(C≡N)], 1605(s) [ν(C=N) of imine], 1495(s) [ν(C=N) of imine], 953(s) [ν(S=O) of DMSO]. UV–vis (DMSO): λ_{max}[nm] (ε_{max}[LM^{-1} cm^{-1}]) = 380 (2.1 × 10^2), 325 (1.4 × 10^4), 310 (1.9 × 10^4). Λ_M (DMSO): 2.05 Ω^{-1}cm^2 M^{-1} (Non-conducting). $\mu_{eff.}/\mu_B$: 1.88 (at 298 K).

Block-shaped X-ray quality yellow single crystals of **1a** were obtained from recrystallization in DMSO.

2.2.2. Preparation of [Cu$_2$(Pbt)$_2$(NCS)$_4$] (2a). About 106 mg (0.5 mM) of Pbt and 97 mg (1.0 mM) of KSCN were taken in 20 mL of MeOH. The solution was colorless. About 185 mg (0.5 mM) of $Cu(ClO_4)_2 \cdot 6H_2O$ was dissolved in 10 mL of MeOH and added dropwise with constant stirring to the ligand solution. At the end of addition, a green solution was obtained and stirring was continued for another 3 h. The resulting reaction mixture after stirring was kept in air for slow evaporation. After two days, a green compound separated, was filtered, washed with 20 mL of diethyl ether, and dried in a vacuum desiccator over fused $CaCl_2$. Yield: 141 mg (72%). $C_{28}H_{16}Cu_2N_8S_6$ (783.21): Anal. Calc for $C_{28}H_{16}Cu_2N_8S_6$: C, 42.90; H, 2.06; N, 14.30; Cu, 16.22. Found: C, 43.06; H, 2.18; N, 14.08; Cu, 15.91%. FTIR (KBr): ν [cm^{-1}]: 2124(vs) [ν(C≡N)], 2092(vs) [ν(C≡N)], 1605(s) [ν(C=N) of imine], 1491(s) [ν(C=N) of imine]. UV–vis (CH_3CN): λ_{max}[nm] (ε_{max}[LM^{-1} cm^{-1}]) = 720 (4.7 × 10^2), 440 (3.4 × 10^3), 325 (2.3 × 10^4), 310 (2.1 × 10^4). Λ_M (acetonitrile): 1.95 Ω^{-1}cm^2 M^{-1} (non-conducting). $\mu_{eff.}/\mu_B$: 1.68 (at 298 K) per Cu atom.

Green rhombohedral single crystals of **2a** suitable for X-ray crystallography were obtained by recrystallization from acetonitrile.

2.3. *Crystal structure determination*

Single crystals of **1a** and **2a** suitable for X-ray structure determination were selected by examination under a microscope and mounted on a Bruker SMART APEX II CCD area detector diffractometer at 293(2) K using graphite monochromated Mo-K$_\alpha$ radiation (λ = 0.71073 Å). Intensity data of **1a** and **2a** were reduced using SAINT [17] and the empirical absorption corrections were performed with SADABS [18]. The structures of **1a** and **2a** were solved by direct methods and refined by full-matrix least-squares based on $|F|^2$ using SHELXL-97 [19]. All non-hydrogen atoms were refined anisotropically. Hydrogens were placed in calculated positions and constrained to ride on their parent. Even the best single crystals employed for data collection imparted diffused diffraction spots. This is indicative of a large mosaic spread. Some of the diffraction spots were overlapping.

Table 1. Crystal data and structure refinement for **1a** and **2a**.

Compound	**1a**	**2a**
Formula	$C_{16}H_{14}CuN_4OS_4$	$C_{28}H_{16}Cu_2N_8S_6$
Formula weight	470.14	783.97
Crystal system	Triclinic	Triclinic
Space group	*P-1*	*P-1*
Unit cell dimensions		
a (Å)	8.799(3)	7.019(3)
b (Å)	9.801(3)	8.710(3)
c (Å)	12.745(4)	13.414(4)
α (°)	109.339(7)	98.895(7)
β (°)	100.513(8)	94.144(7)
γ (°)	101.007(8)	104.633(8)
V (Å^3)	981.6(6)	778.6(5)
Z	2	1
Temperature (K)	293	293
ρ_{Calcd} (g/cm^{-3})	1.591	1.672
μ (Mo-K_α) /mm^{-1}	1.551	1.803
F (000)	478	394
Crystal size (mm)	0.16 × 0.20 × 0.22	0.18 × 0.22 × 0.24
λ (Mo-K_α) (Å)	0.71073	0.71073
θ ranges (°)	$1.8 < \theta < 25.0$	$1.5 < \theta < 25.0$
Total reflection	11,553	7362
Reflection independent (R_{int})	3441 (0.022)	2743 (0.053)
h/k/l	−10:10; −11:11; −14:15	−8:8; −10:10; −15:15
Reflection observed ($I > 2\sigma$)	3028	2039
R_1	0.0634	0.0619
wR_2	0.1757	0.1940
Goodness of fit	1.05	1.09
Largest diff. in peak and hole (e Å^{-3})	3.39 and −0.64	1.03 and −0.72

Notes: $R_1 = \Sigma||F_o| - |F_c||/\Sigma|F_o|$, $wR_2 = [\Sigma w(F_o^2 - F_c^2)^2/\Sigma w(F_o^2)^2]^{1/2}$, Calcd $w = 1/[\sigma^2(F_o^2) + (0.0921P)^2 + 3.0537P]$, where $P = (F_o^{2+}2F_c^2)/3$ for **1a** and $w = 1/[\sigma^2(F_o^2) + (0.0972P)^2 + 1.7649P]$ for **2a**.

Consequently, the integration of those spots could not be performed properly by the processing software. Thus a small portion of the collected reflections was excluded and the final structure was refined using the available data corresponding of θ. However, the reduced data-sets were adequate to give precise structures. All the calculations were carried out using SHELXS-97 [19], SHELXL-97, and SHELXTL [19] programs. The crystallographic data for **1a** and **2a** are summarized in table 1.

2.4. *Computational details*

Computational studies in the present work were done on gas phase geometries of **1a** and **2a** and on their respective linkage isomers. Full geometry optimization for each species without any symmetry restrictions was done using the gradient-corrected DFT level coupled with Becke's exchange functional [20], including the correlation functional of Lee, Yang, and Parr (B3LYP) [21]. The effective core potential (ECP) with basis set LANL2DZ was employed for Cu following the associated valence double ξ basis set of Hay and Wadt [22–24]. The calculations for hydrogen, carbon, nitrogen, oxygen, and sulfur were sufficiently accurate using 6–311G** basis set [25, 26]. Frequency calculations for **1a** and **2a** correspond to real vibrational spectra and thus optimized geometries represent the true energy minima. All the computations in this study were performed by this

LANL2DZ-ECP-6–311G** combination, both basis sets being obtained from basis set exchange (BSE) software and the EMSL Basis Set Library [27, 28]. Gaussian 09, Revision C.01 program package was used for computational purposes [29].

3. Results and discussion

3.1. *Synthesis and formulation*

Pbt was prepared following a reported procedure [30]. Reaction of 1 : 2 : 1 molar proportions of Pbt, KSCN, and $Cu(ClO_4)_2 \cdot 6H_2O$ in DMSO at room temperature gave yellow monomeric $[Cu(Pbt)(NCS)_2DMSO]$ (**1a**) in 68% yield. However, reaction of similar proportions of Pbt, KSCN, and $Cu(ClO_4)_2 \cdot 6H_2O$ in methanol gave the green dimeric thiocyanate bridged $[Cu_2(Pbt)_2(NCS)_4]$ (**2a**) in 72% yield. The C, H, and N microanalytical and copper estimation data of the single crystals of **1a** and **2a** are consistent with our proposed empirical formulas. The complexes are neutral. The room temperature (298 K) effective magnetic moments of **1a** and **2a** are 1.88 and 1.68 μ_B, respectively. These values are consistent with an $S = 1/2$ spin state expected for d^9 systems. A value of 0.350 $cm^3\ M^{-1}\ K$ for $\chi_M T$ was found for **2a** at 298 K, much smaller than the spin-only value of 0.75 $cm^3\ M^{-1}\ K$ expected for a non-interacting $S = 1/2$ spin system, providing evidence of strong antiferromagnetic interactions in **2a**.

3.2. *FTIR spectroscopy*

The IR spectrum of free Pbt shows characteristic vibrations at 1584 and 1456 cm^{-1} [31], due to C=N (pyridyl) and C=N (benzthiazolyl) vibrations, respectively. Both bands in IR spectra **1a** and **2a** shift to higher wavenumbers. For **1a**, those vibrations are at 1605 and 1495 cm^{-1}, respectively, while for **2a**, 1605 and 1491 cm^{-1}. This shift is unusual since binding of C=N to metal centers normally causes a decrease in the stretching frequency of this band, due to formation of a π-back bond from the metal to nitrogen. This dichotomy can be explained in the light of the possible resonance structures of free Pbt [31] (scheme 1).

The structure of Pbt can be considered as a resonance hybrid of three possible canonical forms, A, B, and C. In both ionic forms, B and C, the nitrogen centers are electron rich while sulfur is electron deficient with partial positive charge. Thus, both these forms favor potential N,N-chelation to a hard metal like Cu(II). Our copper(II) compounds, **1a** and **2a**, manifest such preferential chelation with Pbt, where the C=N moieties enjoy partial single bond character. Consequently, the IR frequencies are shifted to higher wavenumbers. This N,N-chelating mode is the only binding mode for Pbt with metal [32, 33]. Diagnostic experimental and calculated (non-scaled) IR frequencies of **1a** and **2a** in Supplementary

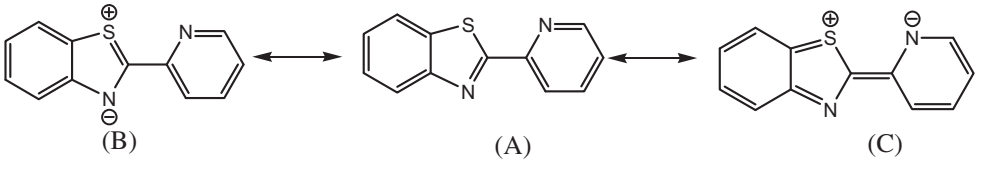

Scheme 1. Some canonical forms of Pbt which contribute to its structure.

Table 2. The diagnostic experimental and calculated IR frequencies for **1a** and **2a**.

Experimental (cm^{-1})	Theoretical (cm^{-1})	Assignments
Complex **1a**		
2101	2106.53	C≡N (oppt. of pyridine moiety)
2080	2069.29	C≡N (oppt. of benzthiazole moiety)
1605	1617.59	C=N (pyridyl)
1495	1539.95	C=N (benzthiazolyl)
952	952.22	S=O
Complex **2a**		
2124	2171.14	C≡N (bridge)
2092	2112.62	C≡N (terminal)
1605	1615.91	C=N (pyridyl)
1491	1533.66	C=N (benzthiazolyl)

material, and their assignments, are tabulated in table 2. The calculated vibrational stretching frequencies of **1a** and **2a** are in good agreement with their experimental data. The experimental and calculated IR spectra of **1a** and **2a** are similar in terms of their band positions, band intensities, and shapes of the bands. Both for **1a** and **2a**, maximum deviations of the computed IR frequencies do not exceed their respective experimental values by 3%. These discrepancies are reasonable, since theoretical calculations are in the gas phase. Thus computed data are often at variance with the experimental [34, 35].

3.3. *Molecular structures*

3.3.1. [Cu(Pbt)(NCS)$_2$DMSO] (1a). The crystal structure (figure 1) of **1a** reveals that the molecular structure is monomeric. Selected metrical parameters for **1a** are given in table 3. The structure shows a 'N_4O' coordination environment of copper. Pbt is a N(pyridyl) and N(benzothiazolyl) donor. The chelate bite angle ∠N3Cu1N4 is 78.46(19)°. Two thiocyanates are nitrogen donors. DMSO offers the lone oxygen donor to copper. The trigonality index (τ) is calculated [36–38]. By definition, $\tau = (\alpha-\beta)/60$, where α and β, respectively, are the largest and second largest angles around the central metal with the surrounded donors. A value of 0 for τ is a perfect square pyramid while unity is observed for a regular trigonal bipyramid. The τ value for **1a** is 0.79 for Cu1. Thus, Cu in **1a** has a distorted trigonal bipyramidal coordination. Two Cu–N bond lengths Cu1–N3 (pyridyl), 2.125(5) Å, and Cu1–N4 (benzothiazole), 1.998(5) Å, are significantly different. However, these values are typical for Cu(II) complexes [31, 39]. For Cu(II) in trigonal bipyramidal environments, Cu–N_{eq}CS bond distance of 1.995(6) Å (range 1.950–2.162 Å) is somewhat longer than that of Cu–N_{ax}CS, 1.919(6) Å (range 1.919–1.958 Å) [9].

Calculated bond parameters by DFT are consistent with the crystallographic data of **1a** given in table 3. The calculated Cu–N bond distances, Cu1–N3 (pyridyl), and Cu1–N4 (benzthiazolyl), are shorter by 0.006 Å and longer by 0.220 Å, respectively, than the experimental data. The calculated chelate bite angle, ∠N3–Cu1–N4, is shorter by 2.26° than the crystallographic data.

3.3.2. [Cu$_2$(Pbt)$_2$(NCS)$_4$] (2a). The molecular structure (figure 2) of **2a** is a dimer of two symmetric thiocyanate bridged copper(II) centers. The two coppers in the dimeric unit of **2a** are coordinatively similar, both five-coordinate with a 'N_4S' chromophore. The bidentate

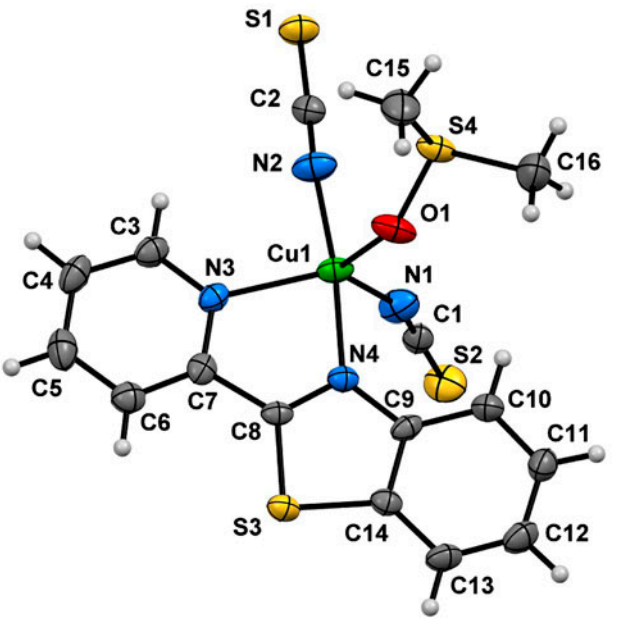

Figure 1. The structure of [Cu(Pbt)(NCS)$_2$DMSO] (**1a**) with ellipsoids at 30% probability.

Table 3. Selected experimental and optimized bond distances (Å) and angles (°) for **1a**.

	Experimental	Optimized
Cu1–O1	2.094(4)	2.252
Cu1–N1	1.995(6)	1.954
Cu1–N2	1.919(6)	1.983
Cu1–N3	2.125(5)	2.119
Cu1–N4	1.998(5)	2.218
N1–C1	1.144(9)	1.184
S2–C1	1.617(7)	1.615
N2–C2	1.146(9)	1.185
S1–C2	1.611(6)	1.615
S4–O1	1.531(4)	1.537
O1–Cu1–N3	113.17(17)	87.5
O1–Cu1–N4	86.50(17)	90.8
O1–Cu1–N1	119.1(2)	97.1
O1–Cu1–N2	95.6(2)	103.1
N1–Cu1–N2	94.0(2)	97.1
N1–Cu1–N3	125.7(2)	170.4
N1–Cu1–N4	90.6(2)	95.3
N2–Cu1–N3	94.8(2)	90.1
N2–Cu1–N4	173.3(2)	159.9
N3–Cu1–N4	78.46(19)	76.2
Cu1–O1–S4	124.6(2)	122.5

Pbt is a N(pyridyl), N(benzothiazolyl) donor. The chelate bite angle, ∠N2Cu2N51, is 80.5(2)°. The apical sulfur in Cu2 comes from S2a of thiocyanate. The Cu2–S2a distance is 2.821(3) Å. Two bridging thiocyanates link through nitrogen and sulfur, while the terminal

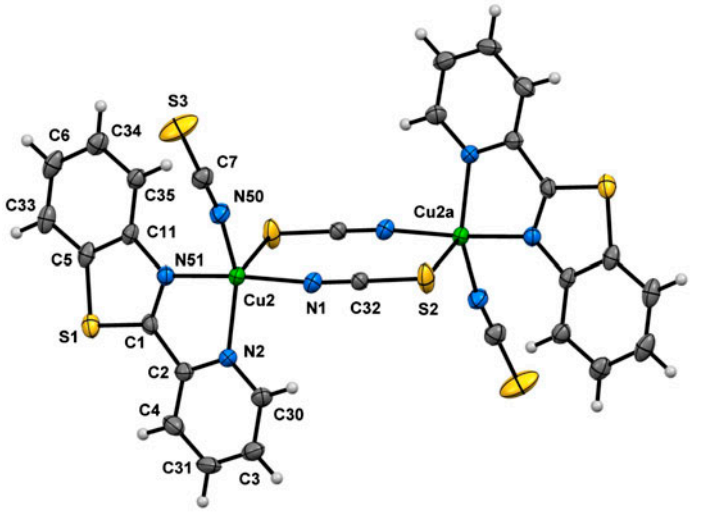

Figure 2. The structure of $[Cu_2(Pbt)_2(NCS)_4]$ (**2a**) with ellipsoids at 30% probability. Symmetry code: (a) $-x$, $1-y$, $-z$.

Table 4. The selected experimental and optimized bond distances (Å) and angles (°) for **2a**.

	Experimental	Optimized		Experimental	Optimized
Cu2–N1	1.939(5)	1.986	N1–Cu2–N2	93.8(2)	90.70
Cu2–N50	1.924(6)	1.945	N1–Cu2–N51	166.5(2)	159.99
Cu2–S2a	2.821(3)	2.853	N2–Cu2–N51	80.5(2)	77.48
S2–C32	1.621(6)	1.634	S2a–Cu2–N50	106.9(2)	98.15
S3–C7	1.612(8)	1.621	S3–C7–N50	179.6(7)	176.19
Cu2–N2	2.034(5)	2.094	N1–Cu2–N50	95.8(2)	94.64
Cu2–N51	2.005(5)	2.171	N2–Cu2–N50	146.7(3)	171.91
N1–C32	1.152(8)	1.174	N50–Cu2–N51	95.5(2)	95.65
N50–C7	1.152(10)	1.181	Cu2–N1–C32	165.8(6)	158.18

Note: a: $-x$, $1-y$, $-z$.

thiocyanate coordinates only through nitrogen to Cu2. In **2a**, the Cu···Cu distance is 5.792 (2) Å [40, 41]. The τ values for Cu2 and Cu2a in **2a** are similar as expected. This is 0.33 for Cu2 [∠N1–Cu2–N5 = 166.5(2) (α) and ∠N2–Cu2-N50 = 146.7(3) (β)]. Thus, the geometries of copper in **2a** are distorted square pyramidal. Selected experimental and theoretical bond lengths and angles of **2a** are summarized in table 4. The two Cu–N bond lengths, Cu2–N2, and Cu2–N51, are 2.034(5) and 2.005(5) Å, respectively. For Cu(II) in square pyramidal environments, the bridging thiocyanate Cu2–N1 is 1.939(5) Å (range 1.950–2.162 Å), somewhat longer than that of terminal thiocyanate Cu2–N50, 1.924(6) Å (range 1.919–1.958 Å) [9].

The packing diagram of **2a** (figure 3) illustrates different π–π stacking interactions. In **2a**, the centroid to centroid separations associated with the pyridine of Pbt are 3.444(2) Å (for rings A and B) and 3.382(3) Å (for rings B and C), indicating stronger intermolecular π–π stacking that stabilizes the configuration of **2a** [42, 43]. The calculated bond parameters of **2a** are comparable with their respective crystallographically determined values in table 4.

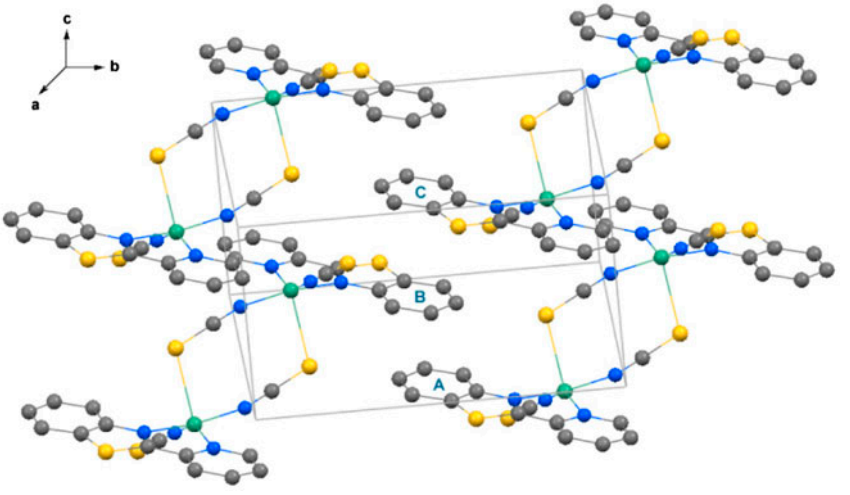

Figure 3. A view of packing diagram of **2a**. Color code: C gray, S yellow, N blue, and Cu green. For the sake of clarity, hydrogens are omitted (see http://dx.doi.org/10.1080/00958972.2013.839784 for color version).

All calculated bond distances in **2a** are higher than their respective experimental values by 0.009–166 Å. The calculated chelate bite angle, ∠N2Cu2N51, is shorter by 3.02° than the X-ray data. These deviations might come from the basis sets which are approximated during calculations or to the influence of the crystal packing on the values of the experimental bond lengths. Theoretical calculations do not consider the effects of chemical environments [44, 45].

3.4. *Electrochemistry*

The redox properties of **1a** and **2a** have been examined in DMSO and acetonitrile, respectively, at GC electrodes under N_2. **1a** exhibits a redox couple on the positive side of the Ag/AgCl reference electrode. The CV of **1a** (Supplementary material) shows a quasi-reversible voltammogram at 0.354 V. The corresponding peak current ratio, i_{pa}/i_{pc} is 1.03. Pbt is electrochemically inert in the potential range of interest, *i.e.* on the positive side of Ag/AgCl [15]. Thus, this oxidation can be assigned as metal centered. Comparison of the voltammetric peak currents with those of the ferrocene–ferrocenium couple under the same experimental conditions establishes that the oxidative responses in **1a** involve one electron which is ascribed to the Cu^{II}/Cu^{III} couple [3]. The dimeric copper(II) complex, **2a**, exhibits two consecutive responses, couple **I** and couple **II**, on the positive side of Ag/AgCl. CV of **2a** (Supplementary material) shows a quasi-reversible oxidation at 0.514 V *versus* Ag/AgCl. The corresponding peak current ratio, i_{pa}/i_{pc} of **I** is 0.77. The second oxidation is discernable at 1.042 V *versus* Ag/AgCl with a peak current ratio, i_{pa}/i_{pc} of 1.89. These results show that the consecutive redox steps are quasi-reversible. Comparison of the voltammetric peak currents with those of the ferrocene–ferrocenium couple under the same experimental conditions establishes that the oxidative responses in **2a** involve one electron in successive steps. Thus the electrochemical response in **2a** is a one-electron, two-step pathway. The electrochemical data for **1a** and **2a** are tabulated in table 5. In general, the

Table 5. Cyclic voltammetric data for **1a** and **2a**.

	Entry	$E_{pa}(i_{pa})$	$E_{pc}(i_{pc})$	$E_{½}$	i_{pa}/i_{pc}
1a		0.462(3.04)	0.246(2.96)	0.354	1.03
2a	Couple-I	0.578(3.72)	0.449(4.86)	0.514	0.77
	Couple-II	1.085(2.71)	0.998(1.43)	1.042	1.89

Notes: E_{pa} = anodic peak potential, V; E_{pc} = cathodic peak potential, V; i_{pa} = anodic peak current, μA; i_{pc} = cathodic peak current, μA; $E_{½} = 0.5\ (E_{pc} + E_{pa})$ V.

peak current, i_p, increases with the square root of scan rate ($v^{1/2}$), but not in proportionality. Thus, the metal centered oxidations for **1a** and **2a** are quasi-reversible [46]. The electrochemical responses for **2a** can be assigned as:

$$Cu^{2+}, Cu^{2+} - e \leftrightarrow Cu^{3+}, Cu^{2+}$$

$$Cu^{3+}, Cu^{2+} - e \leftrightarrow Cu^{3+}, Cu^{3+}$$

These redox assignments of **2a** can be substantiated from a stability consideration of the mixed-valence species, Cu^{3+}, Cu^{2+}. This stability can be expressed in terms of the comproportionation constant (1), K_{con}, where $\Delta E = [E_{1/2}\ (II) - E_{1/2}(I)]$ [47].

$$K_{con} = \frac{[Cu(III)Cu(II)]^2}{[Cu(III)Cu(III)][Cu(II)Cu(II)]} = \exp\left[\frac{nF(\Delta E)}{RT}\right] \quad (1)$$

The larger the separation of the potentials of the couple (ΔE), the greater is the stability of the mixed-valence species with respect to comproportionation. Taking ΔE for **2a** of 0.572 V *versus* SCE (after reference conversion to SCE), the magnitude of the constant K_{con} comes out as 6.9×10^9. This value of K_{con} for **2a** is comparable with those in the literature [47, 48]. Instability of a mixed-valence species under the electrochemical time domain would give a value of 0 for the comproportionation constant, K_{con} [49]. We could not isolate the oxidized species in pure form due to instability at higher potentials. Stabilization of the dicopper(III) complex of (2-pyridyl)alkylamine ligands with halide bridges are well known [50–52]. In our case, five-coordination renders the electro-generated dinuclear Cu (III) species unstable. Such problems were also encountered for electrochemical stabilization of + 3 state of copper in a five-coordinate environment [53]. While examples of five-coordinate species for d^8 systems are not rare [54, 55], most Cu^{3+} complexes are stabilized by peptide, aryl, or arylcorrolato based ligands [56–59]. The separation between the $E_{1/2}$ values of the two couples in **2a** is 528 mV; non-interacting metal centers of similar environments do not have a separation larger than 50 mV [60, 61]. Thus, strong copper–copper interactions in **2a** can induce CV wave splitting by a magnitude of a few hundred mV. Similar separation in CV waves occur in other magnetically coupled binuclear copper (II) complexes [53, 62].

3.5. *Thermal behavior*

The thermal behaviors (TGA and DTA) of **1a** and **2a** have been studied (Supplementary material) from 28.0 to 600.0 °C for **1a** and 32.0–600.0 °C for **2a** in a dynamic nitrogen

atmosphere (flow rate = 20.0 mL/min). About 2.023 mg of **1a** and 4.681 mg of **2a** were heated separately in a platinum crucible at a heating rate of 12.0 °C per minute. Dried and purified α-Al_2O_3 powder was used as a reference. Thermogravimetric (TG) analyzes confirm that **1a** and **2a** are thermally stable up to 100 and 200 °C, respectively. Thermograms of **1a** and **2a** show sequential events of weight loss. For **1a** (Supplementary Material), up to 164 °C, the experimental mass loss of 16.33% agrees with theoretical loss (16.62%) for removal of one DMSO per formula unit. Loss of DMSO in copper(II) compounds is known to occur within the temperature range [63, 64]. The corresponding DTA curve is exothermic. Beyond 200 °C, there is a characteristic and steady weight loss in the TG curve accompanied with a sharp upward DTA curve, showing that the corresponding heat change is highly exothermic, likely due to compound combustion. Up to 450 °C, the experimental mass loss of 68.89% is in proximity to the theoretical loss (69.84%) for removal of one Pbt along with two thiocyanates. The combustion is virtually complete at 550 °C. The final residue corresponds to the metallic copper (theoretical loss: 13.53%; experimental loss: 13.33%). The TG curve (Supplementary Material) for **2a** shows mass losses in two distinct steps. The first loss from 200 to 260 °C is due to liberation of four thiocyanates exothermally (theoretical loss: 29.62%; experimental loss: 31.11%). From 300 to 400 °C, the experimental loss of 54.44% corroborates with theoretical loss of 54.11% due to the removal of two Pbt per formula unit. The corresponding DTA plot is exothermic.

3.6. *BVS analysis*

To assign the oxidation state of each copper in **1a** and **2a**, we have done bond valence sum (BVS) calculations [65–68]. In this method, the valence '*s*' of a bond between two atoms *i* and *j* is related by an empirical expression (2), where r_{ij} is the length of the bond (expressed in Å) and

$$S_{ij} = \exp[(r_0 - r_{ij})/0.37] \tag{2}$$

r_0 a parameter characteristic of the bond. This r_0, known as bond valence parameter, is however geometry and coordination number specific. The oxidation number N_i of atom *i* is simply the algebraic sum of these '*s*' values of all the bonds (*n*) around the atom, *i* (3).

$$N_i = \Sigma_{i=1}^{n} S_{ij} \tag{3}$$

Thus, if r_0 is known for a particular bond type, the BVS can be calculated from crystallographically determined r_{ij} values. The r_0 values for Cu^{2+}–N (1.719 Å), Cu^{2+}–O (1.679 Å) and Cu^{2+}–S (2.024 Å) were taken from the literature [69]. Taking the crystallographically determined bond lengths in Å of four Cu–N bonds and one Cu–O bond in **1a**, the BVS for copper is 2.270 valence units (table 6). Similar calculations for **2a** give BVS of 2.132 (table 6). These results corroborate the stipulated error limit of ± 0.25 as proposed earlier by Thorp [70, 71]. Thus an oxidation number of + 2 can safely be assigned to each copper in **1a** and **2a**.

3.7. *Theoretical considerations*

For our current model studies, we have undertaken four probable linkage isomers (**1a**, **1b**, **1c**, and **1d**) for the monomeric copper(II) compound and three isomers (**2a**, **2b**, and **2c**)

Table 6. Bond valence values for individual copper centers in **1a** and **2a**.

Compound	Bond type	Bond distance (Å)	Bond valence	Bond valance sum for individual copper
1a	Cu1–O1	2.132	0.294	2.270
	Cu1–N4	2.134	0.326	
	Cu1–N5	1.989	0.482	
	Cu1–N6	1.965	0.514	
	Cu1–N8	1.876	0.654	
2a	Cu2–N1	1.939	0.552	2.132
	Cu2–N2	2.034	0.427	
	Cu2–N50	1.924	0.575	
	Cu2–N51	2.005	0.462	
	Cu2–S2_a	2.821	0.116	

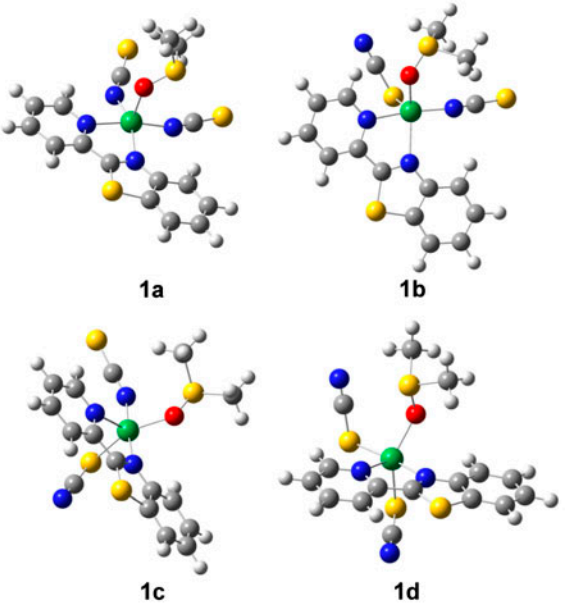

Figure 4. Optimized geometries of **1a** and its other thiocyanate linkage isomers. Color code: C gray, H white, N blue, O red, S yellow, and Cu green (see http://dx.doi.org/10.1080/00958972.2013.839784 for color version).

for the dimeric copper(II) compound [44]. The geometries were optimized in doublet (monomer) and triplet (dimer) state using the DFT method with the B3LYP functional. The optimized structures are shown in figures 4 and 5, respectively, for the monomeric and the dimeric complexes. The optimized energies of all the possible linkage isomers for the monomeric and the dimeric copper(II) complexes are summarized in table 7. The geometry optimization of all the probable geometries of the monomeric complexes reveal that **1a** is more stable than **1b**, **1c**, and **1d**, respectively, by 6.97, 21.28, and 44.42 kJ/mol of energy. Similar geometry optimization shows that **2a** is more stable than **2b** and **2c** linkage isomers of our dimeric copper(II) compound by 29.94 and 44.41 kJ/mol, respectively. Here, we have been able to isolate and crystallize **1a** and **2a** naturally. Thus, the current theoretical outcomes corroborate our experimental results.

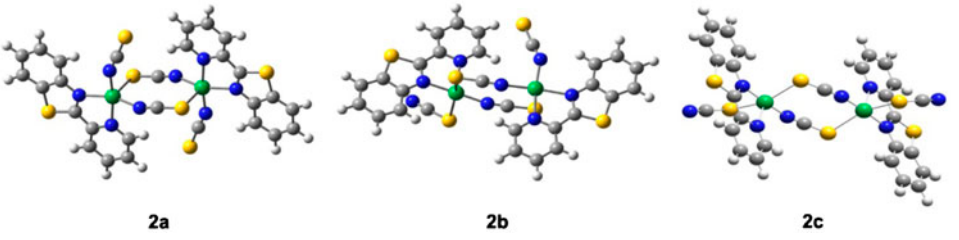

Figure 5. Optimized geometries of **2a** and its thiocyanate linkage isomers. Color code: C gray, H white, N blue, S yellow, and Cu green (see http://dx.doi.org/10.1080/00958972.2013.839784 for color version).

Table 7. Geometrical optimization energies of various linkage isomers of copper complexes calculated at the level of DFT.

Linkage isomers	*E* (Hartree)	Δ*E* (kJ/M)
[Cu(Pbt)$(NCS)_2$(DMSO)]		
1a	−2701.5809772	0.00
1b	−2701.5783207	6.97
1c	−2701.5728706	21.28
1d	−2701.5640589	44.42
[$Cu_2(Pbt)_2(NCS)_4$]		
2a	−4296.6747830	0.00
2b	−4296.6633779	29.94
2c	−4296.6578671	44.41

4. Conclusion

We have synthesized and characterized two paramagnetic copper(II) thiocyanato complexes, [Cu(Pbt)$(NCS)_2$(DMSO)] (**1a**) and [$Cu_2(Pbt)_2(NCS)_4$] (**2a**), from the diimine based 2-(2-pyridinyl)-benzthiazole (Pbt). **1a** is monomeric, while **2a** is a symmetrical thiocyanate bridged dimer. Electrochemical studies of **2a** reveal that the two Cu(II) centers are quasi-reversibly oxidized to Cu(III) in two successive one-electron pathways. Theoretical calculations at the DFT level show that the geometries of the linkage isomers, **1a** and **2a**, are the most stable. BVS calculations were also undertaken to assign the oxidation state of each copper centers in **1a** and **2a**.

To augment our conclusion, we can compare our complexes with two other recent copper–thiocyanato complexes. One is a mixed-valence Cu^ICu^{II} coordination polymer having two modes of thiocyanate bridging, $\mu_{1,3}$-SCN and $\mu_{1,1,3}$-SCN [72]. The former $\mu_{1,3}$-SCN bridging mode is akin to **2a**. **1a** is devoid of any thiocyanate bridging. However, the other mode, $\mu_{1,1,3}$-SCN, connecting three copper centers is rare [72]. Due to the simultaneous presence of these two kinds of bridges, this mixed-valence copper complex adopts a unique 2-D supramolecular sheet structure with inter-sheet π-π stacking interaction. Consequently, this Cu^ICu^{II} assembly represents a rare situation where magnetic coupling has been mediated through π-π stacking and the bridging coordination modes of thiocyanate. The other copper-thiocyanate system is a copper(I) coordination polymer with $\mu_{1,3}$-SCN bridging mode supported by the ancillary ligand, bis(4-phenylpyrazol-1-yl)methane (phpzm) [73]. This copper(I) assembly displays promising photophysical properties. In this perspective, the prospect of copper-thiocyanate systems is immense.

Supplementary material

CCDC 915999 and 911197 contain the supplementary crystallographic data for **1a** and **2a**, respectively. These data can be obtained free of charge via http://www.ccdc.cam.ac.uk/conts/retrieving.html, or from the Cambridge Crystallographic Data Center, 12 Union Road, Cambridge CB2 1EZ, UK; Fax: (+44) 1223-336-033; or E-mail: deposit@ccdc.cam.ac.uk.

Acknowledgments

Financial support [F. No. SR/FT/CS-75/2010] received from the SERC under Department of Science and Technology (DST), India, is gratefully acknowledged. J.P.N. gratefully acknowledges the University Grants Commission (UGC), New Delhi, India, for financial support [F. No. 41-220/2012 (SR)].

References

[1] L.-H. Gao, M. Guan, K.-Z. Wang, L.-P. Jin, C.-H. Huang. *Eur. J. Inorg. Chem.*, **2006**, 3731 (2006).
[2] C. Mock, I. Puscasu, M.J. Rauterkus, G. Tallen, J.E.A. Wolff, B. Krebs. *Inorg. Chim. Acta*, **319**, 109 (2001).
[3] P.U. Maheswari, M. van der Ster, S. Smulders, S. Barends, G.P. van Wezel, C. Massera, S. Roy, H. den Dulk, P. Gamez, J. Reedijk. *Inorg. Chem.*, **47**, 3719 (2008).
[4] X. Chen, F.J. Femia, J.W. Babich, J. Zubieta. *Inorg. Chim. Acta*, **314**, 91 (2001).
[5] S. Tzanopoulou, I.C. Pirmettis, G. Patsis, C. Raptopoulou, A. Terzis, M. Papadopoulos, M. Pelecanou. *Inorg. Chem.*, **45**, 902 (2006).
[6] S. Haneda, Z. Gan, K. Eda, M. Hayashi. *Organometallics*, **26**, 6551 (2007).
[7] D.M. Cropek, A. Metz, A.M. Müller, H.B. Gray, T. Horne, D.C. Horton, O. Poluektov, D.M. Tiede, R.T. Weber, W.L. Jarrett, J.D. Phillips, A.A. Holder. *J. Chem. Soc., Dalton Trans.*, 13060 (2012).
[8] J. Gangopadhyay, S. Sengupta, S. Bhattacharyya, I. Chakraborty, A. Chakravorty. *Inorg. Chem.*, **41**, 2616 (2002).
[9] J.L. Burmeister. *Coord. Chem. Rev.*, **105**, 77 (1990).
[10] M. Kabešová, R. Boča, M. Melník, D. Valigura, M. Dunaj-Jurčo. *Coord. Chem. Rev.*, **140**, 115 (1995).
[11] X.F. He, C.M. Vogels, A. Decken, S.A. Westcott. *Polyhedron*, **23**, 155 (2004).
[12] S.-Z. Hu, D. Shi, T. Huang, J. Wan, Z. Huang, J. Yang, C. Xu. *Inorg. Chim. Acta*, **173**, 1 (1990).
[13] M. Maji, P. Sengupta, S.K. Chattopadhyay, G. Mostafa, C.H. Schwalbe, S. Ghosh. *J. Coord. Chem.*, **54**, 13 (2001).
[14] B.K. Panda, K. Ghosh, S. Chattopadhyay, A. Chakravorty. *J. Organomet. Chem.*, **674**, 107 (2003).
[15] E.K. Beloglazkina, I.V. Yudin, A.G. Majouga, A.A. Moiseeva, A.I. Tursina, N.V. Zyk. *Russ. Chem. Bull., Int. Ed.*, **55**, 1803 (2006).
[16] W.C. Wolsey. *J. Chem. Educ.*, **50**, A335 (1973).
[17] SAINT Plus. *Data Reduction and Correction Program*, v. 6.01., Bruker AXS, Madison, Wisconsin, USA (1998).
[18] SADABS v. 2.01. *Bruker/Siemens Area Detector Absorption Correction Program*., Bruker AXS, Madison, Wisconsin, USA (1998).
[19] G.M. Sheldrick. *Acta Crysallogr., Sect. A*, **64**, 112 (2008).
[20] A.D. Becke. *Phys. Rev. A*, **38**, 3098 (1988).
[21] C. Lee, W. Yang, R.G. Parr. *Phys. Rev. B*, **37**, 785 (1988).
[22] P.J. Hay, W.R. Wadt. *J. Chem. Phys.*, **82**, 270 (1985).
[23] P.J. Hay, W.R. Wadt. *J. Chem. Phys.*, **82**, 284 (1985).
[24] P.J. Hay, W.R. Wadt. *J. Chem. Phys.*, **82**, 299 (1985).
[25] K. Raghavachari, J.S. Binkley, R. Seeger, J.A. Pople. *J. Chem. Phys.*, **72**, 650 (1980).
[26] A.D. McLean, G.S. Chandler. *J. Chem. Phys.*, **72**, 5639 (1980).
[27] D. Feller. *J. Comput. Chem.*, **17**, 1571 (1996).
[28] K.L. Schuchardt, B.T. Didier, T. Elsethagen, L. Sun, V. Gurumoorthi, J. Chase, J. Li, T.L. Windus. *J. Chem. Inf. Model.*, **47**, 1045 (2007).
[29] Gaussian 09, Revision C.01, M.J. Frisch, G.W. Trucks, H.B. Schlegel, G.E. Scuseria, M.A. Robb, J.R. Cheeseman, G. Scalmani, V. Barone, B. Mennucci, G.A. Petersson, H. Nakatsuji, M. Caricato, X. Li, H.P. Hratchian, A.F. Izmaylov, J. Bloino, G. Zheng, J.L. Sonnenberg, M. Hada, M. Ehara, K. Toyota, R. Fukuda, J. Hasegawa, M. Ishida, T. Nakajima, Y. Honda, O. Kitao, H. Nakai, T. Vreven, J.A. Montgomery, Jr., J.E. Peralta, F. Ogliaro, M. Bearpark,

J.J. Heyd, E. Brothers, K.N. Kudin, V.N. Staroverov, R. Kobayashi, J. Normand, K. Raghavachari, A. Rendell, J. C. Burant, S.S. Iyengar, J. Tomasi, M. Cossi, N. Rega, J.M. Millam, M. Klene, J.E. Knox, J.B. Cross, V. Bakken, C. Adamo, J. Jaramillo, R. Gomperts, R.E. Stratmann, O. Yazyev, A.J. Austin, R. Cammi, C. Pomelli, J.W. Ochterski, R.L. Martin, K. Morokuma, V.G. Zakrzewski, Ö. Farkas, J.B. Foresman, J.V. Ortiz, J. Cioslowski, D.J. Fox. Gaussian, Inc., Wallingford CT (2009).
[30] A.K. Chakraborti, S. Rudrawar, K.B. Jadhav, G. Kaur, S.V. Chankeshwara. *Green Chem.*, **9**, 1335 (2007).
[31] K. Marjani, M. Mousavi, D.L. Hughes. *Transition Met. Chem.*, **34**, 85 (2009).
[32] S. Sengupta, J. Gangopadhyay, A. Chakravorty. *J. Chem. Soc., Dalton Trans.*, 4635 (2003).
[33] R. Czewieniec, A. Kapturkiewiez, J. Lipkowski. *Inorg. Chim. Acta*, **358**, 2701 (2005).
[34] S. Majumder, A. Bhattacharya, J.P. Naskar, P. Mitra, S. Chowdhury. *Inorg. Chim. Acta*, **399**, 166 (2013).
[35] B. Machura, A. Świtlicka, M. Penkala. *Polyhedron*, **45**, 221 (2012).
[36] S. Chowdhury, N. Koshino, A. Canlier, K. Mizuoka, Y. Ikeda. *Inorg. Chim. Acta*, **359**, 2472 (2006).
[37] A.W. Addision, T.N. Rao, J. Reedijik, J.V. Rijin, G.C. Verschoor. *J. Chem. Soc., Dalton Trans.*, 1349 (1984).
[38] M. Li, A. Ellern, J.H. Espenson. *Inorg. Chem.*, **44**, 3690 (2005).
[39] L. Yanmei, C. Yongheng, O. Zhibin, C. Shi, Z. Chuxiong, L. Xueyi. *Chin. J. Chem.*, **30**, 303 (2012).
[40] J.A.R. Navarro, M.A. Romero, J.M. Salas, M. Quirós, E.R.T. Tiekink. *Inorg. Chem.*, **36**, 4988 (1997).
[41] Z.-L. You, P. Hou, C. Wang. *J. Coord. Chem.*, **62**, 593 (2009).
[42] M.-X. Li, H. Wang, S.-W. Liang, M. Shao, X. He, Z.-X. Wang, S.-R. Zhu. *Cryst. Growth Des.*, **9**, 4626 (2009).
[43] R.P. Sharma, A. Saini, S. Singh, P. Venugopalan, W.T.A. Harrison. *J. Fluorine Chem.*, **131**, 456 (2010).
[44] H. Golchoubian, S. Koohzad, M. Ramzani, D. Farmanzadeh. *Polyhedron*, **51**, 1 (2013).
[45] S. Majumder, J.P. Naskar, S. Banerjee, A. Bhattacharya, P. Mitra, S. Chowdhury. *J. Coord. Chem.*, **66**, 1178 (2013).
[46] R. Greef, R. Peat, L.M. Peter, D. Pletcher, J. Robinson. *Instrumental Methods in Electrochemistry*, p. 188, Ellis Horwood Limited, England (1985).
[47] S.K. Mondal, L.K. Thompson, K. Nag, J.P. Charland, E.J. Gabe. *Inorg. Chem.*, **26**, 1391 (1987).
[48] W. Zhang, S. Liu, C. Ma, D. Jiang. *Polyhedron*, **17**, 3835 (1998).
[49] S.K. Mandal, K. Nag. *Inorg. Chem.*, **22**, 2567 (1983).
[50] B.J. Hathaway, *Comprehensive Coordination Chemistry*, G.Wilkinson (Ed.), Pergamon, New York (1987), pp. 533–774.
[51] T. Osako, K.D. Karlin, S. Itoh. *Inorg. Chem.*, **44**, 410 (2005).
[52] S. Shit, U. Yadava, D. Saha, R. Fröhlich. *J. Coord. Chem.*, **66**, 66 (2013).
[53] J.P. Naskar, B. Guhathakurta, L. Lu, M. Zhu. *Polyhedron*, **43**, 89 (2012).
[54] A.R. Rossi, R. Hoffman. *Inorg. Chem.*, **14**, 365 (1975).
[55] J.E. Huheey, E.A. Keiter, R.L. Keiter. *Inorganic Chemistry*, 4th Edn, p. 479, Harper Collins College Publishers, New York (1993).
[56] M. Suzuki. *Acc. Chem. Res.*, **40**, 609 (2007).
[57] A. Pratesi, P. Zanello, G. Giorgi, L. Messori, F. Laschi, A. Casini, M. Corsini, C. Gabbiani, M. Orfei, C. Rosani, M. Ginanneschi. *Inorg. Chem.*, **46**, 10038 (2007).
[58] L.M. Huffman, S.S. Stahl. *J. Chem. Soc., Dalton Trans.*, 8959 (2011).
[59] C. Brückner, R.P. Briñas, J.A. Krause Bauer. *Inorg. Chem.*, **42**, 4495 (2003).
[60] F. Ammar, J.M. Saveant. *J. Electroanal. Chem.*, **47**, 115 (1973).
[61] J.B. Flamagan, S. Margel, A.J. Bard, F.C. Anson. *J. Am. Chem. Soc.*, **100**, 4248 (1978).
[62] P.S. Zacharias, A. Ramachandraiah. *Polyhedron*, **4**, 1013 (1985).
[63] D.-X. Xue, J.-B. Lin, J.-P. Zhang, X.-M. Chen. *Cryst. Eng. Comm.*, **11**, 183 (2009).
[64] D. Sun, Y. Ke, T.M. Mattox, B.A. Ooro, H.-C. Zhou. *Chem. Commun.*, **2005**, 5447 (2005).
[65] I.D. Brown. *Chem. Soc. Rev.*, **7**, 359 (1978).
[66] D. Altermatt, I.D. Brown. *Acta Crystallogr., Sect. B*, **41**, 240 (1985).
[67] I.D. Brown. *Acta Crystallogr., Sect. B*, **48**, 553 (1992).
[68] I.D. Brown, D. Altermatt. *Acta Crystallogr., Sect. B*, **41**, 244 (1985).
[69] I.D. Brown. *Chem. Soc. Rev.*, **109**, 6858 (2009).
[70] H.H. Thorp. *Inorg. Chem.*, **31**, 1585 (1992).
[71] W. Liu, H.H. Thorp. *Inorg. Chem.*, **32**, 4102 (1993).
[72] R.-Z. Wei, J.-M. Shi, W. Wei, S.-L. Liu. *J. Coord. Chem.*, **66**, 1916 (2013) and references cited therein.
[73] H.-Y. Li, Z.-L. Xu, H.-X. Li, Y. Zhang, L.-X. Dai, J.-P. Lang. *J. Coord. Chem.*, **65**, 4203 (2012).